Journal of Power Sources 211 (2012) 12–18

Contents lists available at SciVerse ScienceDirect

Journal of Power Sources

journal homepage: www.elsevier.com/locate/jpowsour

A combined first-principles computational/experimental study on $LiNi_{0.66}Co_{0.17}Mn_{0.17}O_2$ as a potential layered cathode material

José J. Saavedra-Arias [a,b,c], Chitturi Venkateswara Rao [a], Jifi Shojan [b], Ayyakkannu Manivannan [d], Lorraine Torres [b], Yasuyuki Ishikawa [a,*], Ram S. Katiyar [b,**]

[a] Department of Chemistry and The Chemical Physics Graduate Program, University of Puerto Rico, San Juan, PR 00931, USA
[b] Department of Physics and Institute for Functional Nanomaterials, University of Puerto Rico, San Juan, PR 00931, USA
[c] Department of Physics, Universidad Nacional, Heredia 40101, Costa Rica
[d] Energy Systems Dynamics Division, Department of Energy, Morgantown, WV 26507, USA

ARTICLE INFO

Article history:
Received 28 November 2011
Received in revised form
6 February 2012
Accepted 11 February 2012
Available online 19 February 2012

Keywords:
Lithium-ion batteries
Layered cathode
First-principles calculations
Capacity

ABSTRACT

First-principles calculations are used to analyze the phase stability, formation energy, and Li intercalation potential for a series of layered cathode materials. The calculations show $LiNi_{0.66}Co_{0.17}Mn_{0.17}O_2$ as a promising cathode for lithium-ion batteries. The layer-structured $LiNi_{0.66}Co_{0.17}Mn_{0.17}O_2$ is prepared via wet chemical route, followed by annealing at 1123 K and characterized using powder X-ray diffraction, scanning electron microscopy, and X-ray photoelectron spectroscopy. The characterization techniques reveal single-phase $LiNi_{0.66}Co_{0.17}Mn_{0.17}O_2$ with highly ordered structure. Galvanostatic charge–discharge curves recorded at 1C show the discharge capacity of ca. 167 mAh g^{-1} and good cyclic performance for 25 cycles.

© 2012 Elsevier B.V. All rights reserved.

1. Introduction

Lithium-ion batteries with high energy and power densities are actively pursued for different applications as power tools, electric vehicle (EV), and hybrid electric vehicle (HEV) applications. Considerable effort has been expended to seek for a new cathode material as an alternative to the extant $LiCoO_2$ that suffers from drawbacks – its toxicity, high cost, and low rechargeable capacity [1–7]. In this regard, materials based on Ni and Mn has become especially important. $LiNiO_2$ showed initial discharge capacity of ~200 mAh g^{-1}, but it exhibits a phase transformation in the voltage range of 3–4.5 V [8,9]. $LiMnO_2$ cathode material is difficult to synthesize in a $R\bar{3}m$ phase, and also shows a structural transformation from layered to spinel structure upon repeated electrochemical cycling [10,11]. The combination of Co, Ni, and Mn in a layered metal oxide structure ($R\bar{3}m$) gives a range of compositions $Li[Ni_ACo_BMn_C]O_2$ ($A + B + C = 1$), and it had been reported that the capacity obtained depends upon the composition, synthesis methodology, and charge–discharge limits [3,5,12,13]. One of the prominent cathode materials is $LiNi_{1/3}Co_{1/3}Mn_{1/3}O_2$, which was introduced by Ohzuku and Makimura in 2001 [14]. This material exhibits superior electrochemical properties than $LiCoO_2$ in terms of high discharge capacity [15–18]. Ceder and co-workers [19] performed a combined computational/experimental study on $Li_xNi_{1/3}Co_{1/3}Mn_{1/3}O_2$. They concluded that the redox couples in this compound are Co^{3+}/Co^{4+}, Ni^{3+}/Ni^{4+}, and Ni^{2+}/Ni^{3+}, if the lithium content (x) is in the range of $0 \le x \le 1/3$, $1/3 \le x \le 2/3$, and $2/3 \le x \le 1$, respectively. The material showed a specific capacity of ~185 mAh g^{-1} during the first cycle and a stable behavior after 16 charge–discharge cycles. Although it exhibit high discharge capacity, the electrochemical performance of $LiNi_{1/3}Co_{1/3}Mn_{1/3}O_2$ is known to deteriorate slowly due to the cationic mixing between nickel and lithium ion at 3b crystallographic site of the $Li[Ni_ACo_BMn_C]O_2$ lattice [16].

Following this metal oxide composition, Dahn and co-workers [16] synthesized $LiNi_xCo_{1-2x}Mn_xO_2$ ($0 \le x \le 1/2$) cathode material by the mixed hydroxide method. The discharge capacities of these materials were found between 110 and 130 mAh g^{-1} in the voltage range of 3.0–4.2 V. Other approach in this field was the increase in Ni content ($0.5 < A < 1.0$) in $Li[Ni_ACo_BMn_C]O_2$. Cao et al. [12] synthesized $LiNi_{0.6}Co_{0.2}Mn_{0.2}O_2$ by co-precipitation method and observed a specific capacity of 151 mAh g^{-1} after 50 cycles in the

* Corresponding author. Tel.: +1 787 764 0000x5908; fax: +1 787 756 7717.
** Corresponding author. Tel.: +1 787 751 4210; fax: +1 787 764 2571.
E-mail addresses: yishikawa@uprrp.edu (Y. Ishikawa), rkatiyar@uprrp.edu (R.S. Katiyar).

0378-7753/$ – see front matter © 2012 Elsevier B.V. All rights reserved.
doi:10.1016/j.jpowsour.2012.02.029

range of 2.8–4.3 V at 0.4C rate. Cho et al. [20,21] investigated $LiNi_{0.8}Co_{0.1}Mn_{0.1}O_2$ as a potential candidate to substitute $LiCoO_2$. However, this composition also suffers from drawbacks such as LiOH and Li_2CO_3 impurity phases, and cationic mixing. Sun et al. [22,23] investigated core-shell structured materials with bulk composition of $LiNi_{0.8}Co_{0.1}Mn_{0.1}O_2$ as cathode and reported the high discharge capacity of 209 mAh g^{-1} and an extended cycle life of 500 cycles. All these experimental results accumulated over the years indicate that the transition metals in appropriate composition with highly ordered structure exhibit good electrochemical performance.

The objective of the present work is to identify a superior layered cathode material for Li-ion rechargeable batteries. Our approach is of a theory-guided design in the spirit of Ceder et al. [6,19], in which we vary the composition of the cathode materials and examine their relative formation energy/stability using first-principles calculations. In the initial step, $LiNiO_2$ was considered as the basic material and the alloyed material $LiNi_{(1-x-y)}Co_xMn_yO_2$ formed by substitution of Ni by Co and Mn was computationally scrutinized to elucidate a composition with the most favorable formation energy/stability. The computationally identified layered cathode material, $LiNi_{0.66}Co_{0.17}Mn_{0.17}O_2$, is then synthesized and characterized experimentally.

2. Theoretical and experimental

2.1. Computational methodology

First-principles calculations were performed in the local density approximation (LDA) to density-functional theory (DFT) as implemented in the Vienna Ab Initio Simulation Package (VASP) [24,25]. The wave functions were expanded in plane waves with kinetic energy cut-off value of 400 eV. All calculations were performed with spin polarization. The reciprocal-space k-point grid was $3 \times 3 \times 3$ and 12 formula units were used which is equivalent to 48 atoms. The super-cell had up to 12 transition metal positions for the substitutions. The study of the different 'solid solution' was performed under a systematic and randomized substitution of the transition metal atom. All possible transition metal arrangements for single, double substitutions have been calculated and part of the possible arrangements in the triple and quadruple substitutions has been calculated. In order to reduce the number of the plane waves required for simulating the interactions between ions and electrons, ultrasoft (US) Vanderbilt pseudopotentials [26] have been used. All structures were fully relaxed with respect to external and internal parameters. The Li atoms were removed one by one until full delithiation of the crystal in a several different arrangements. The substitution of the transition metal atoms was performed by equivalent position replacement to minimize the energy of the system. The present computational study does not include the Hubbard U to improve the accuracy of the voltage prediction for cathode materials [27]. In this work, a systematic computational study within the LDA framework is conducted to depict a transition metal 'solid solution' that may be used as new cathode material for secondary lithium-ion batteries.

2.2. Experimental details

Lithium nitrate [$LiNO_3$], nickel nitrate hexahydrate [$Ni(NO_3)_2 \cdot 6H_2O$], manganese nitrate [$Mn(NO_3)_2 \cdot 6H_2O$], cobalt nitrate hexahydrate [$Co(NO_3)_2 \cdot 6H_2O$], and citric acid [$H_3C_6H_5O_7$] as starting materials to prepare $LiNi_{0.66}Co_{0.17}Mn_{0.17}O_2$ in a wet chemical route. In a typical procedure, 7.4335 g $LiNO_3$, 19.7065 g $Ni(NO_3)_2 \cdot 6H_2O$, 4.3814 g $Mn(NO_3)_2 \cdot 6H_2O$ and 5.0801 g $Co(NO_3)_2 \cdot 6H_2O$ were dissolved in distilled water and then 16.9935 g citric acid was added as chelating agent. Five percent of extra lithium was added to compensate its evaporation at high annealing temperature. Subsequently, the solution was heated at 353 K until a transparent sol was obtained. The resulting gel precursor was dried at 393 K overnight and calcined at 773 K for 4 h to remove the organic impurities. Finally, the sample was sintered at 1123 K in air for 12 h.

2.3. Characterization techniques

XRD measurements were performed on a PANalytical X'Pert Pro powder diffractometer using a Cu Kα source operated at a scan rate of 3° min^{-1} over the 2θ range of 15–75°. Scanning electron microscopic (SEM) images were recorded using a JEOL JSM-6480LV system operated with an accelerating voltage of 20 kV. X-ray photoelectron spectroscopy (XPS) measurements were performed using PHI5600 ESCA system Physical Electronics.

The electrochemical performance of the synthesized material was examined in two electrode CR2032 type coin cell configuration using liquid electrolyte consisting of 1 M $LiPF_6$ dissolved in 1:2 (v/v) mixture of ethylene carbonate (EC) and dimethyl carbonate (DMC). The working electrode was prepared by

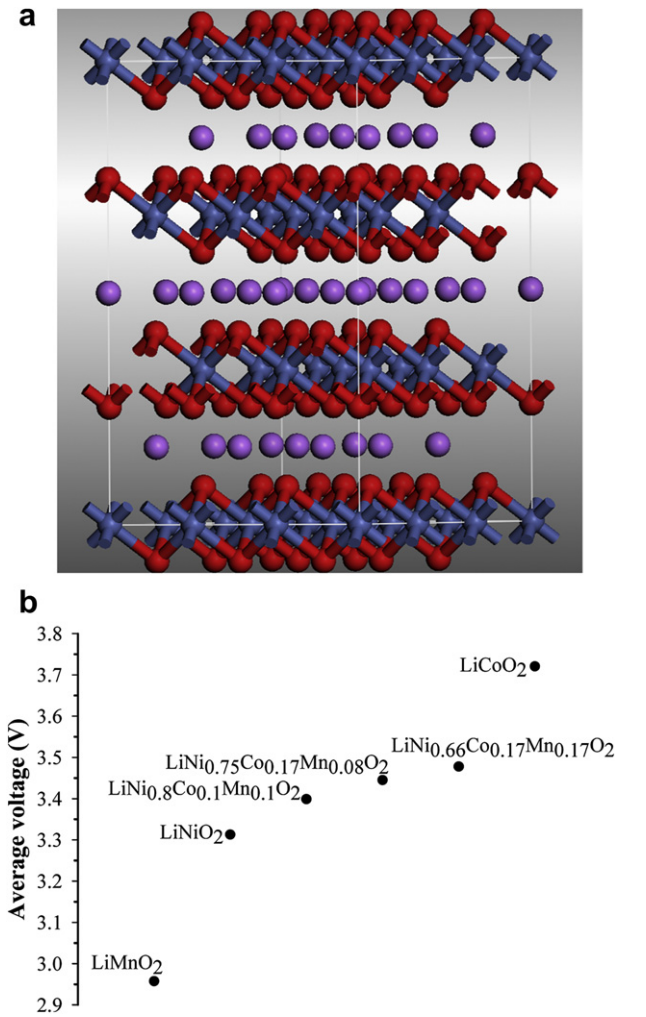

Fig. 1. (a) Schematic representation of $LiMO_2$ (M = transition metal) and (b) average voltage for different layered cathode materials.

mixing $LiNi_{0.66}Co_{0.17}Mn_{0.17}O_2$ powder, polyvinylidine fluoride, and carbon black in 80:10:10 weight ratio [28,29]. The slurry was prepared using N-methyl pyrrolidone (NMP) as solvent, spread on Al foil, and kept for drying at about 353 K for 24 h. Li metal foil was used as anode and Celgard 2400 was used as separator between anode and cathode. The coin cell was assembled inside the Ar-filled glove box (MBraun, O_2 and $H_2O < 1$ ppm). The loading of active material was 6 mg cm^{-2}. The electrochemical measurements were performed on a computer controlled potentiostat, Gamry Instruments Inc. Galvanostatic charge–discharge measurements were carried out in the voltage range 2.5–4.5 V at room temperature.

3. Results and discussion

3.1. Computational

The calculations are initiated by constructing a layered structure (space group, $R\bar{3}m$) with parameters: $a = b = 2.67$ Å, $c = 14.59$ Å, $\beta = 90°$ and $x = 0.254$ [24]. The layered structure is shown in Fig. 1a. It depicts the occupation of lithium at 3b site, transition metals at 3a site, and oxygen at 6c site. Average voltage values for various cathode materials are calculated using the expression [30,31]: $\langle V \rangle = -\Delta G_r/(x_2 - x_1)F$ where ΔG_r is the Gibbs free energy for the reaction ($MO_2 + Li \rightarrow LiMO_2$), F is Faraday's constant, and x_2 and x_1 are the limits of lithium content in the Li_xMO_2 structure. The determined values are shown in Fig. 1b. As can be seen, $LiMnO_2$ and $LiCoO_2$ show the lowest (2.96 V) and highest (3.72 V) average voltage, respectively. The computed voltage of $LiCoO_2$ is similar to the literature reports [30,31]. Augmenting substitution of Ni by Co and Mn in $LiNiO_2$ showed the increase in the average voltage (Fig. 1b). According to the results, $LiNi_{0.66}Co_{0.17}Mn_{0.17}O_2$ showed the highest average voltage for the transition metal substitution compounds.

The interactions between the lithium, oxygen, and transition metals ions were analyzed and the formation energy of the solid solution was examined. The computed formation energies of the transition metals in Li-layered structure have been obtained by the expression, $\Delta E_{mix} = E(LiNi_{(1-x-y)}Co_xMn_yO_2) - (1-x-y)E(LiNiO_2) - xE(LiCoO_2) - yE(LiMnO_2)$ [32]. If ΔE_{mix} is negative, the arrangement of the elements in the compound is in a random and equivalent position, to form a solid solution. A positive ΔE_{mix} indicates that it is difficult to form the solid solution because of likely local phase segregation. However, the systems with small positive formation energy can also be synthesized due to the entropic factors, which favor the mixed state at high temperature. The relative formation energy results, upon Co substitution in $LiNiO_2$ (not showing here), suggest that materials with 8–33% of Co in $LiNiO_2$ can be synthesized and it is in agreement with several experimental results [33–37]. Formation energy of the materials with different amounts of transition metals is shown in Fig. 2a. As can be seen, the three compositions show negative ΔE_{mix}, which suggests a strongly bound arrangement on each composition. Among them, $LiNi_{0.8}Co_{0.1}Mn_{0.1}O_2$ is the most stable compound at full lithiation. If the lithium cathode material maintains a layered structure, up to 50% of Li atoms may be removed to keep the reversibility of the Li-ion battery [38,39]. Therefore, phase stability of the materials is computed with compositions $Li_{0.5}Ni_{0.8}Co_{0.1}Mn_{0.1}O_2$,

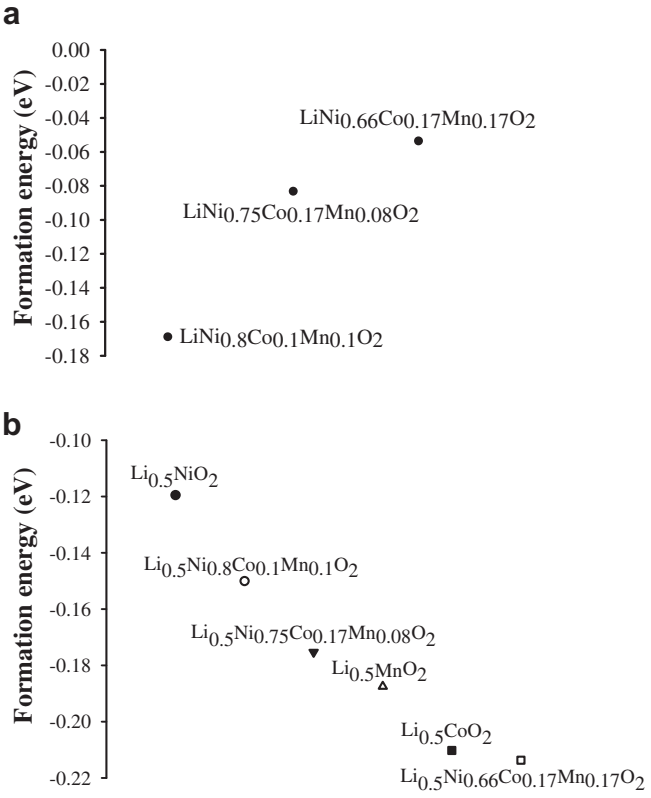

Fig. 2. (a) Formation energy for three different alloy cathode materials and (b) stability of different layered cathode material at half of the Li content.

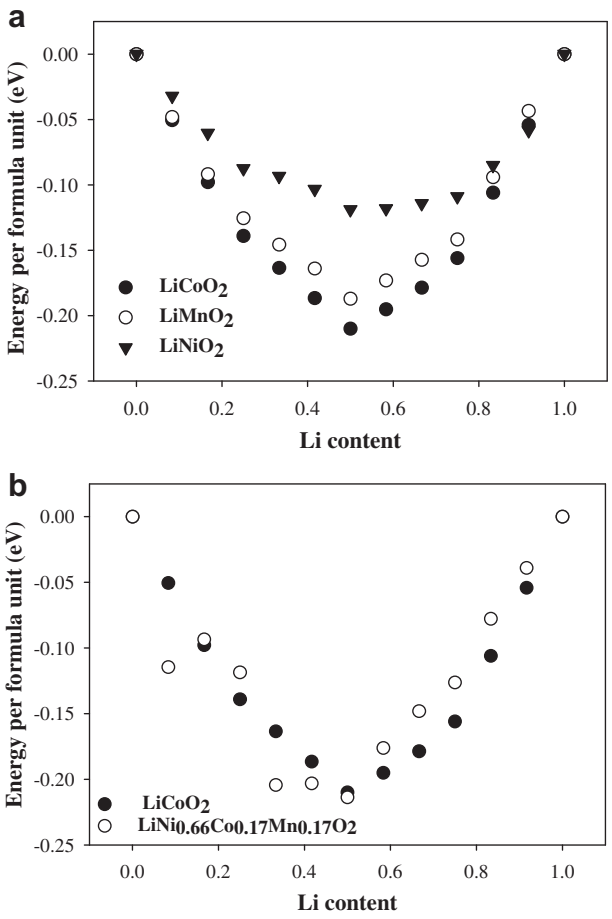

Fig. 3. (a) Relative formation energy for $LiMO_2$ (M = Co, Mn, and Ni) and (b) relative formation energy of Li_xCoO_2 and $Li_xNi_{0.66}Co_{0.17}Mn_{0.17}O_2$ ($0 \le x \le 1$).

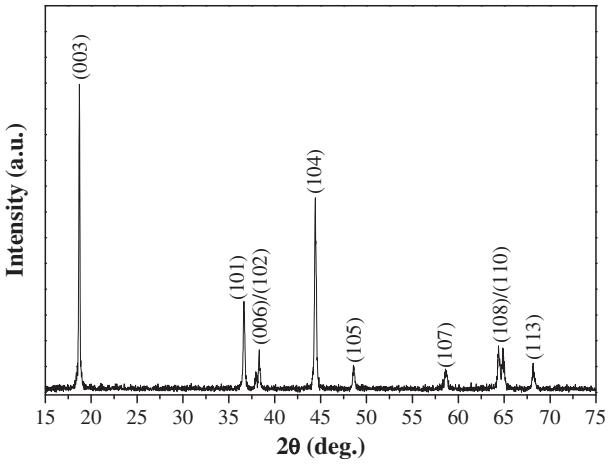

Fig. 4. Powder XRD pattern for the annealed $LiNi_{0.66}Co_{0.17}Mn_{0.17}O_2$ at 1123 K: scan rate of 3° min^{-1}.

$Li_{0.5}Ni_{0.75}Co_{0.17}Mn_{0.08}O_2$, and $Li_{0.5}Ni_{0.66}Co_{0.17}Mn_{0.17}O_2$. The results are shown in Fig. 2b. Although the fully lithiated $LiNi_{0.8}Co_{0.1}Mn_{0.1}O_2$ has a large formation energy compared to $LiNi_{0.66}Co_{0.17}Mn_{0.17}O_2$, this material displays less stability at 50% lithium extraction. Among the investigated materials, $LiNi_{0.66}Co_{0.17}Mn_{0.17}O_2$ exhibited higher stability up to 50% of the lithium extraction. Based on the calculated average voltage and formation energy, $LiNi_{0.66}Co_{0.17}Mn_{0.17}O_2$ seems to be a promising candidate for lithium-ion battery.

Phase stability of the layered structure upon delithiation was also studied. The simulation studies are carried out with fully optimized structures. The results obtained are plotted in Fig. 3. A convex behavior is revealed. It is indicating the stability of each intermediate state in the lithium extraction process. These results confirm that, $LiCoO_2$ is more stable than the other two cathode materials $LiMO_2$ (M = Ni and Mn). To study the phase stability process on $LiNi_{0.66}Co_{0.17}Mn_{0.17}O_2$, structures with Ni–Co–Mn distribution arrangements were constructed. The $LiNi_{0.66}Co_{0.17}Mn_{0.17}O_2$ arrangement that minimizes the total energy was selected for the study. However, the selected one does not show a fully convex behavior from 0 to 0.5 of the Lithium extraction. Although the system that minimizes the energy was used, the difference in total energy among those arrangements is up to approximately 0.033 eV, suggesting that, any of the other transition metal arrangements may show a fully convex behavior for the study. Fig. 3b shows the relative formation energies of the partially delithiated Li_xCoO_2 and $Li_xNi_{0.66}Co_{0.17}Mn_{0.17}O_2$ intermediate compounds as a function of the lithium content ($0 < x < 1$). The

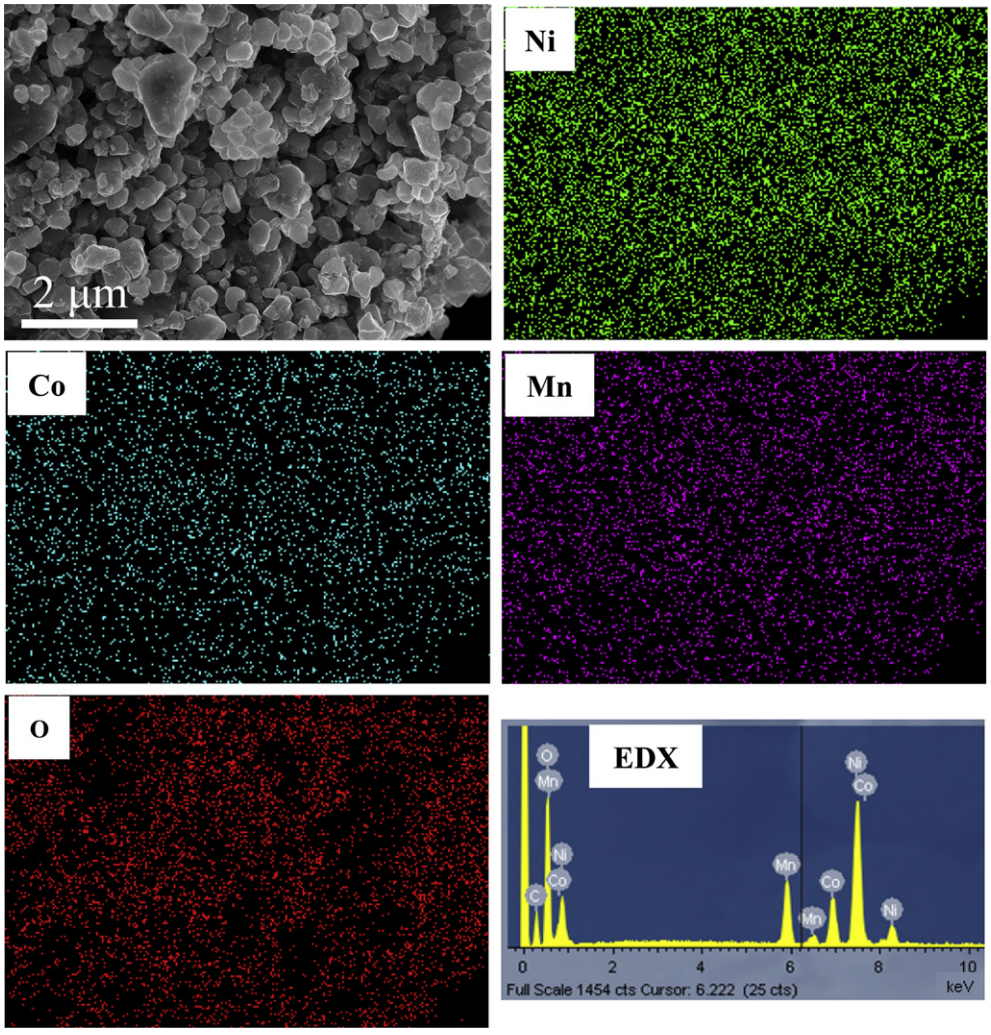

Fig. 5. SEM image with EDX mapping of elements in the annealed $LiNi_{0.66}Co_{0.17}Mn_{0.17}O_2$.

results show that the substitution of Ni by Co and Mn lowers the relative formation energy of the Li_xNiO_2 as the lithium extraction proceeds. Moreover, $LiNi_{0.66}Co_{0.17}Mn_{0.17}O_2$ is showing similar convex behavior as $LiCoO_2$, which is the most popular commercial cathode material. According to the negative formation energy (−0.0535 eV), average voltage (3.48 V), and similar phase stability upon lithium extraction compared to $LiCoO_2$, $LiNi_{0.66}Co_{0.17}Mn_{0.17}O_2$ is a promising layered cathode material for lithium-ion batteries.

3.2. Experimental

The as-synthesized $LiNi_{0.66}Co_{0.17}Mn_{0.17}O_2$ was characterized using XRD and the spectrum is shown in Fig. 4. All the diffraction lines are well indexed in the rhombohedral system with $R\bar{3}m$ space group. As seen in Fig. 4, both the (0 0 6)/(1 0 2) and (1 0 8)/(1 1 0) doublets are well separated. It clearly indicates a good hexagonal ordering of layered $LiNi_{0.66}Co_{0.17}Mn_{0.17}O_2$ [40–42]. XRD patterns reveal a single-phase α-$NaFeO_2$-type structure for the samples calcined at 1123 K.

To predict the hexagonal ordering of the sample, r_I-factor was calculated using the expression: $r_I\text{-factor} = (I_{006} + I_{102})/I_{101}$ [43,44]. The r_I-factor is 0.695, indicates highly ordered structure. In addition, the integrated intensity ratio of (0 0 3) and (1 0 4) peaks, which is considered as a sensitive parameter to determine the cationic distribution in the α-$NaFeO_2$-type lattice, is determined. In general, the ratio I_{003}/I_{104} less than 1.2 indicate the undesirable cationic mixing [13]. For the sample annealing at 1123 K, the I_{003}/I_{104} is 1.583, implying the negligible cationic mixing in the sample. Surface morphology of the $LiNi_{0.66}Co_{0.17}Mn_{0.17}O_2$ is assessed by SEM. The corresponding electronic image with EDX mapping for all the elements is shown in Fig. 5. Agglomerated polyhedral-shaped particles ca. 1–2 μm in size are observed. The EDX mapping images depicted the homogeneous distribution of respective elements in the material. EDX spectrum confirms the presence of respective elements.

The XPS results in Fig. 6 indicate that the O1s spectrum exhibited a major peak at 530.8 eV and a shoulder at 528.4 eV, suggesting that the Ni-rich micro-domains are dominantly present compared with Mn-rich ones in the matrix [45]. The binding energy of Mn $2p_{3/2}$ electron is 641.7 eV, which is closed to the binding energy of Mn $2p_{3/2}$ electron (641.7 eV) in Li_2MnO_3, where the manganese oxidation state is 4+. A weak shoulder peak at 641 eV corresponds to Mn^{3+} in the material [46,47]. For Co $2p_{3/2}$ electron, its binding energy is 779.3 eV which matches with the reported results (779.3–779.9 eV) for Co in 3+ oxidation state [15,47,48]. In the case of Ni, the recorded XPS spectra show a characteristic satellite peak around 860.2 eV in addition to the main Ni $2p_{3/2}$ peak centered at 854.3 eV. Such a satellite peak is also observed due to the multiple splitting in the energy level of the Ni-containing oxides, NiO, $LiNiO_2$ and $LiMn_{1.5}Ni_{0.5}O_4$ [47,49]. The binding energy of Ni $2p_{3/2}$ electron observed at 854.3 eV is in agreement with the value reported for Ni^{2+} in $LiMn_{1.5}Ni_{0.5}O_4$. A weak shoulder peak observed at 860.2 eV for Ni $2p_{3/2}$ is reported in the literature for Ni^{3+} in Ni_2O_3 XPS [50]. A minor contribution of Ni^{3+} and Mn^{3+} may be due to the electron transfer between the ion-pairs leading to small amount of valency-degeneracy. The present XPS results imply that the predominant oxidation states of Ni, Co, and Mn in the $LiNi_{0.66}Co_{0.17}Mn_{0.17}O_2$ are 2+, 3+ and 4+, respectively.

To study the rate capability of the fabricated electrodes, the cells were charged and discharged at 1C rate in the voltage range between 2.5 and 4.5 V, and the corresponding galvanostatic charge–discharge curves are shown in Fig. 7a. The initial charge and discharge capacities observed for the $LiNi_{0.66}Co_{0.17}Mn_{0.17}O_2$ at 1C are 213 and 167 mAh g^{-1}, respectively. The extended cyclic stability

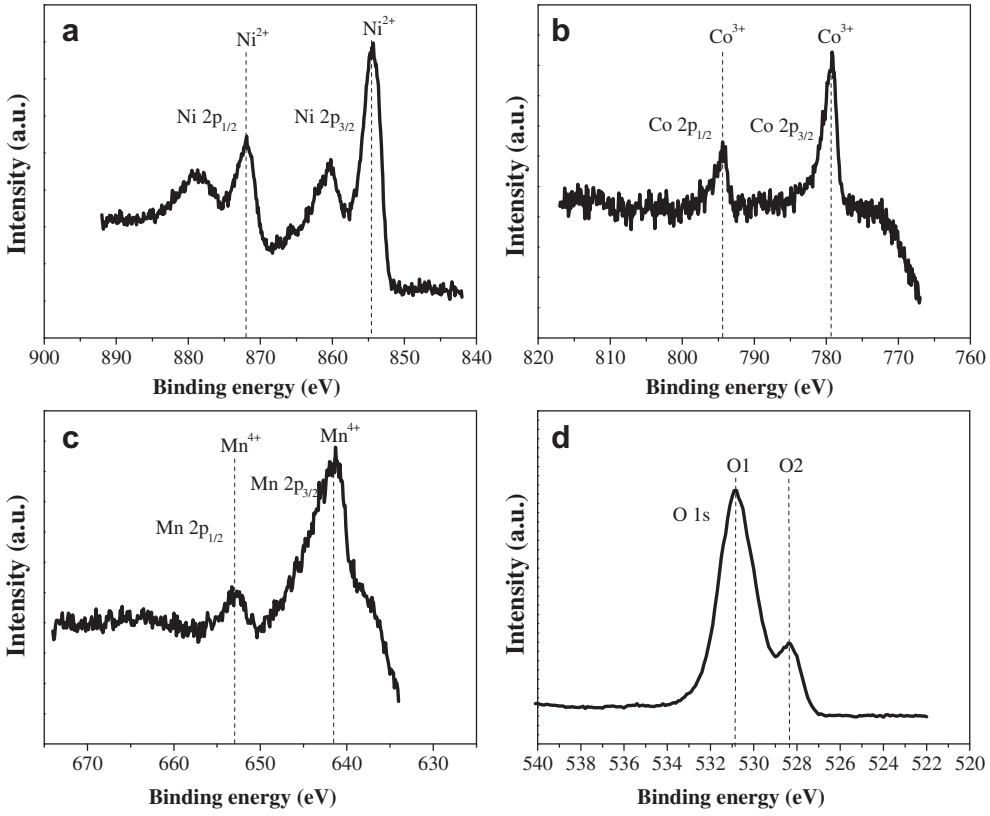

Fig. 6. X-ray photoelectron spectra for the annealed $LiNi_{0.66}Co_{0.17}Mn_{0.17}O_2$.

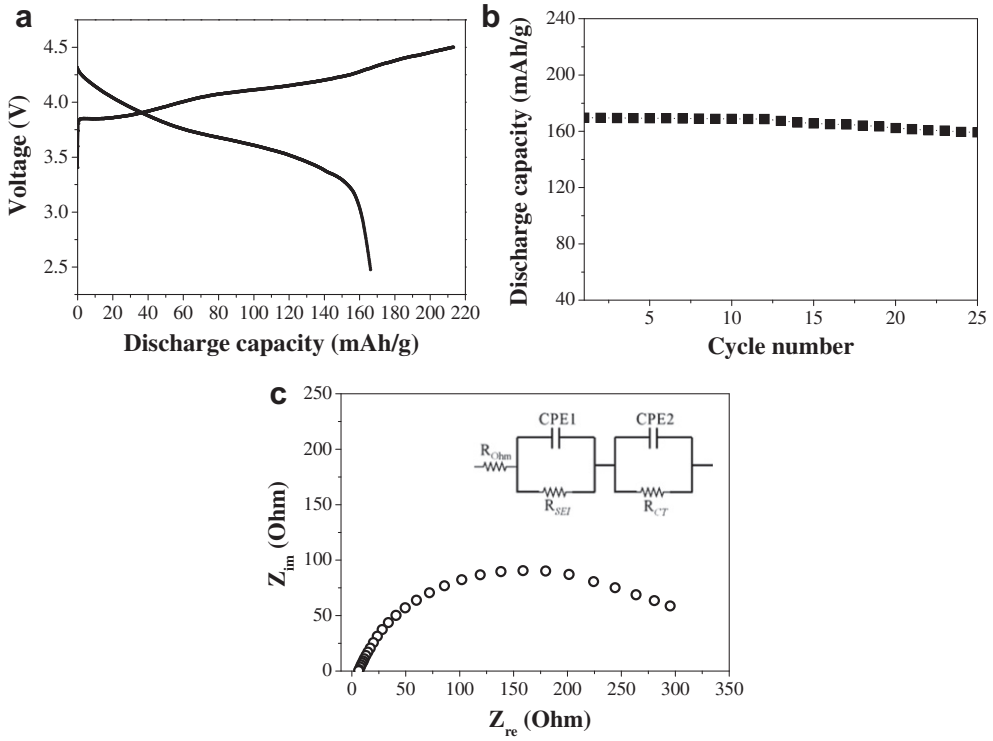

Fig. 7. (a) First charge/discharge cycle for $LiNi_{0.66}Co_{0.17}Mn_{0.17}O_2$ at 1C between 2.5 and 4.5 V; (b) cycling performance of $LiNi_{0.66}Co_{0.17}Mn_{0.17}O_2$ at 1C for 25 cycles; and (c) AC impedance spectrum in the frequency range from 100 kHz to 0.01 Hz (inset in the figure shows the equivalent circuit for the EIS measurement).

measurements of $LiNi_{0.66}Co_{0.17}Mn_{0.17}O_2$ electrode conducted at 1C rate for 25 cycles are shown in Fig. 7b. As can be seen, $LiNi_{0.66}Co_{0.17}Mn_{0.17}O_2$ exhibited a stable capacity during the first 12 cycles and a slow deterioration in the capacity is observed further. The material delivered initial discharge capacity of 169.7 mAh g^{-1} at room temperature and the discharge capacity falls to 165.6, 162.3, and 159.3 mAh g^{-1} after 15th, 20th, and 25th cycles. It indicates that the nominal capacity of $LiNi_{0.66}Co_{0.17}Mn_{0.17}O_2$ is retained with 93.8% after 25 cycles. AC impedance measurements are carried out after five charge–discharge cycles at 1C, and the corresponding Nyquist plot is shown in Fig. 7c. The impedance plots show a high-frequency intercept at the Z_{re} axis and a broad depressed semicircle. The high-frequency intercept is due to the Ohmic resistance (R_{ohm}). The depressed semicircle in the high-frequency and low-frequency regions is related to the formation of a surface layer on the active material and the intercalation/deintercalation of lithium ions into/from the electrodes. An equivalent circuit used to fit the spectra is shown in the inset. The parameters, R_{SEI} and CPE1, correspond to the surface layer resistance and capacitance, whereas R_{CT} and CPE2 correspond to the lithium intercalation/deintercalation process and interfacial capacitance, respectively [17]. The R_{CT} is calculated to be 205 ohm for the pristine $LiNi_{0.66}Co_{0.17}Mn_{0.17}O_2$ electrode. Further studies are underway to improve the performance by fabricating electrodes with either the sub-micron sized particles or metal oxide-based composite or protective-layer-coated metal oxide.

4. Conclusions

Theoretical calculations reveal good average voltage, negative formation energy, and phase stability for $LiNi_{0.66}Co_{0.17}Mn_{0.17}O_2$. This computationally identified material was synthesized using wet chemical route and characterized. The electrochemical measurements performed on $LiNi_{0.66}Co_{0.17}Mn_{0.17}O_2$ reveal the good discharge capacity of ca. 167 mAh g^{-1} and good capacity retention at 1C. The results suggest that $LiNi_{0.66}Co_{0.17}Mn_{0.17}O_2$ is a possible cathode material for high power lithium-ion batteries.

Acknowledgments

Financial supports from the NASA-CANM (Grant # NNX08BA48A), NASA-EPSCoR (Grant # NNX08AB12A) and the Institute for Functional Nanomaterials (IFN) are acknowledged. We thank the High Performance Computing Facility (HPCF) at University of Puerto Rico for providing us with computing resources, and continual support from UPR materials characterization center (MCC). Fruitful discussions with Dr. Naba K. Karan and Dr. Gurpreet Singh are also acknowledged.

References

[1] M. Armand, J.-M. Tarascon, Nature 451 (2008) 652.
[2] M.S. Whittingham, Chem. Rev. 104 (2004) 4271.
[3] V. Etacheri, R. Marom, R. Elazari, G. Salitra, D. Aurbach, Energy Environ. Sci. 4 (2011) 3243.
[4] B.L. Ellis, K.T. Lee, L.F. Nazar, Chem. Mater. 22 (2010) 691.
[5] A. Manthiram, A.V. Murugan, A. Sarkar, T. Muraliganth, Energy Environ. Sci. 1 (2008) 621.
[6] G. Ceder, MRS Bull. 35 (2010) 693.
[7] Y.S. Meng, M.E. Arroyo-de Dompablo, Energy Environ. Sci. 2 (2009) 589.
[8] T. Ohzuku, A. Ueda, M. Nagayama, J. Electrochem. Soc. 140 (1993) 1862.
[9] H. Arai, S. Okada, Y. Sakurai, J.-I. Yamaki, Solid State Ionics 95 (1997) 275.
[10] J. Paterson, A.R. Armstrong, P.G. Bruce, J. Electrochem. Soc. 151 (2004) A1552.
[11] M.M. Thackeray, S.-H. Yang, A.J. Kahaian, K.D. Kepler, E. Skinner, J.T. Vaughey, S.A. Hackney, Electrochem. Solid-State Lett. 1 (1998) 7.
[12] H. Cao, Y. Zhang, J. Zhang, B. Xia, Solid State Ionics 176 (2005) 1207.
[13] R. Santhanam, B. Rambabu, J. Power Sources 195 (2010) 4313.
[14] T. Ohzuku, Y. Makimura, Chem. Lett. 30 (2001) 642.
[15] Z. Lu, D.D. MacNeil, J.R. Dahn, Electrochem. Solid-State Lett. 4 (2001) A200.
[16] D.D. MacNeil, Z. Lu, J.R. Dahn, J. Electrochem. Soc. 149 (2002) A1332.
[17] Ch. Venkateswara Rao, A. Leela Mohana Reddy, Y. Ishikawa, P.M. Ajayan, ACS Appl. Mater. Interfaces 3 (2011) 2966.
[18] N. Yabuuchi, T. Ohzuku, J. Power Sources 119–121 (2003) 171.
[19] B.J. Hwang, Y.W. Tsai, D. Carlier, G. Ceder, Chem. Mater. 15 (2003) 3676.
[20] J. Cho, Y.-W. Kim, B. Kim, J.-G. Lee, B. Park, Angew. Chem. Int. Ed. 42 (2003) 1618.

[21] J. Eom, M.G. Kim, J. Cho, J. Electrochem. Soc. 155 (2008) A239.
[22] Y.-K. Sun, S.-T. Myung, B.-C. Park, J. Prakash, I. Belharouak, K. Amine, Nat. Mater. 8 (2009) 320.
[23] S.-T. Myung, K.-S. Lee, D.-W. Kim, B. Scrosati, Y.-K. Sun, Energy Environ. Sci. 4 (2011) 935.
[24] G. Kresse, J. Furthmüller, Phys. Rev. B 54 (1996) 11169.
[25] S.K. Mishra, G. Ceder, Phys. Rev. B 59 (1999) 6120.
[26] D. Vanderbilt, Phys. Rev. B 41 (1990) 7892.
[27] F. Zhou, M. Cococcioni, C.A. Marianetti, D. Morgan, G. Ceder, Phys. Rev. B 70 (2004) 235121.
[28] N. Santander, S.R. Das, S.B. Majumder, R.S. Katiyar, Surf. Coat. Tech. 177–178 (2004) 60.
[29] J.J. Saavedra-Arias, N.K. Karan, D.K. Pradhan, A. Kumar, S. Nieto, R. Thomas, R.S. Katiyar, J. Power Sources 183 (2008) 761.
[30] M.K. Aydinol, A.F. Kohan, G. Ceder, J. Power Sources 68 (1997) 664.
[31] M.K. Aydinol, A.F. Kohan, G. Ceder, K. Cho, J. Joannopoulos, Phys. Rev. B 56 (1997) 1354.
[32] D. de Fontaine, in: H. Ehrenreich, D. Turnbull (Eds.), Solid State Physics, vol. 47, Academic Press, 1994, pp. 33–176.
[33] J.J. Saavedra-Arias, R. Thomas, N.K. Karan, Y. Ishikawa, R.S. Katiyar, ECS Trans. 16 (2009) 9.
[34] H.W. Tang, Z.H. Zhu, Z.R. Chang, Z.J. Chen, X.Z. Yuan, H. Wang, Electrochem. Solid State Lett. 11 (2008) A34.
[35] Z.X. Yang, B. Wang, W.S. Yang, X. Wei, Electrochim. Acta 52 (2007) 8069.
[36] R.V. Chebiam, F. Prado, A. Manthiram, J. Electrochem. Soc. 148 (2001) A49.
[37] J. Cho, G. Kim, H.S. Lim, J. Electrochem. Soc. 146 (1999) 3571.
[38] K. Mizushima, P.C. Jones, P.J. Wiseman, J.B. Goodenough, Mater. Res. Bull. 15 (1980) 783.
[39] K. Mizushima, P.C. Jones, P.J. Wiseman, J.B. Goodenough, Solid State Ionics 3–4 (1981) 171.
[40] X. Zhang, W.J. Jiang, A. Mauger, Qilu, F. Gendron, C.M. Julien, J. Power Sources 195 (2010) 1292.
[41] R.P. Gravereau, C. Delmas, J. Electrochem. Soc. 143 (1996) 1168.
[42] K.S. Park, M.H. Cho, S.J. Jin, K.S. Nahm, Electrochem. Solid-State Lett. 7 (2004) A239.
[43] J.R. Dahn, U. von Sacken, C.A. Michal, Solid State Ionics 44 (1990) 87.
[44] J.N. Reimers, E. Rossen, C.D. Jones, J.R. Dahn, Solid State Ionics 61 (1993) 335.
[45] Y.-J. Shin, W.-J. Choi, Y.-S. Hong, S. Yoon, K.S. Ryu, S.H. Chang, Solid State Ionics 177 (2006) 515.
[46] D. Li, Y. Sasaki, K. Kobayakawa, Y. Sato, Electrochim. Acta 51 (2006) 3809.
[47] K.M. Shaju, G.V. Subba Rao, B.V.R. Chowdari, Electrochim. Acta 48 (2002) 145.
[48] S. Madhavi, G.V.S. Rao, B.V.R. Chowdari, S.F.Y. Li, J. Electrochem. Soc. 148 (2001) A1279.
[49] J.G. Li, L. Wang, Q. Zhang, X.M. He, J. Power Sources 189 (2009) 28.
[50] Y. Sun, C. Ouyang, Z. Wang, X. Huang, L. Chen, J. Electrochem. Soc. 151 (2004) A504.